Magnetic anisotropy in Li-phosphates and origin of magnetoelectricity in $LiNiPO_4$

Kunihiko Yamauchi and Silvia Picozzi*
CASTI Regional Laboratory, Consiglio Nazionale delle Ricerche—Istituto Nazionale di Fisica della Materia (CNR-INFM), 67100 L'Aquila, Italy

(Received 7 August 2009; revised manuscript received 17 November 2009; published 21 January 2010)

Li-based phosphates are paradigmatic materials for magnetoelectricity. By means of first-principles calculations, we elucidate the microscopic origin of spin anisotropy and of magnetoelectric effects in $LiNiPO_4$. The comparison with $LiCoPO_4$ reveals that Co d^7 and Ni d^8 electronic clouds show distinct orbital shapes, which in turn result in an opposite trend of the local spin anisotropy with respect to the surrounding O_6 cages. Due to magnetic anisotropy, the Ni-based phosphate shows a peculiar "angled-cross" spin ground state, which is responsible for magnetoelectricity. In this respect, we show that, under a magnetic field H_x, an electronic polarization P_z arises, with an estimated linear magnetoelectric coefficient in good agreement with experiments.

DOI: 10.1103/PhysRevB.81.024110 PACS number(s): 75.80.+q, 75.30.Gw, 75.50.Ee

I. INTRODUCTION

Olivine phosphates $LiCoPO_4$ and $LiNiPO_4$ are attracting large interests, due to their peculiar magnetoelectric (ME) effect [i.e., the control of ferroelectric (magnetic) properties via a magnetic (electric) field] as well as their application for electrodes in rechargeable Li batteries.[1,2] Recently, ferrotoroidic domains and antiferromagnetic domains have been independently observed in $LiCoPO_4$ by using second harmonic generation.[3] The toroidal moment, generated by a vortex of magnetic moments, is considered as source of a novel *ferroic order*, closely related to ME effects[4,5] as well as to multiferroicity[6] (i.e., coexistence of long-range magnetic and dipolar orders). In fact, $LiCoPO_4$ shows a nonzero linear ME coefficient, α_{xy} and α_{yx}, at low temperature, consistent with the toroidal moment T nearly parallel to z axis,[5] whereas $LiNiPO_4$ shows α_{xz} and α_{zx}.[7] The difference in the nonzero tensor element is related to the spin direction: In $LiCoPO_4$, antiferromagnetic (AFM) spins have been found to be along the b axis[8] or uniformly rotated from this axis by 4.6°,[9] whereas in $LiNiPO_4$, it has been proposed the collinear AFM spins to lie along the c axis.[10]

Magnetoelectricity has been investigated by means of Landau theory.[9,11] For example, Chupis[11] explained the origin of the "butterfly" ME hysteresis loop, experimentally observed[12,13] a few degrees below T_N, on the basis of an angled-cross-type spin configuration (consistent with neutron diffraction data, suggesting magnetic moments to be close to collinear along the c axis in $LiNiPO_4$). The ME hysteresis loop was successfully explained by the transition from an angled-cross state to a weak ferromagnetic state under a magnetic field of the order of one tesla, by using the Landau free-energy formalism. Besides, note that the linear ME effect, observed in Ref. 13 for $T \leq T_N$, can exist only in the angled-cross spin configuration. Yet, the microscopic origin as well as the magnitude of the ME effect in phosphates has not been clarified in terms of first principles calculations.

In this paper, within density-functional theory (DFT) we investigate the magnetic anisotropy for Li phosphates $LiTMPO_4$(TM=Ni,Co) and we are able to correlate the orbital degree of freedom with the calculated anisotropy and spin configuration. The discussion on magnetic anisotropy is particularly important for $LiNiPO_4$, where we find, as magnetic ground state, a peculiar spin-cross configuration that leads to magnetoelectricity; finally, we clarify the microscopic origin of ME effects, our calculated ME coefficient being in quantitative agreement with experiments.

II. METHODOLOGY AND STRUCTURAL DETAILS

DFT simulations were performed using the VASP code[14] and the PAW pseudopotentials[15] within the GGA+U formalism[16] (U=5 eV and J=0 eV for Ni d states). Other values of U=2 and 8 eV were also tested. The cutoff energy for the plane wave expansion of the wave functions was set to 400 eV and a **k**-point shell of (2, 4, 4) was used for the Brillouin zone integration. Lattice parameters were fixed as experimentally observed.[9,17] The internal atomic coordinates were fully optimized in a (fully compensated) AFM configuration, keeping $S_1=S_2=-S_3=-S_4$ configuration. In the orthorhombic $Pnma(D_{16}^{2h})$ paramagnetic space group, these four Co/Ni sites are related by eight symmetry operations; all the rotations and mirror reflections accompany translations, so that the Co/Ni sites are slightly deviated from high-symmetry positions. Optimized coordinates of the four Co/Ni ions are: Co1/Ni1$(1/4+\epsilon,1/4,-\delta)$, Co2/Ni2$(3/4+\epsilon,1/4,1/2+\delta)$, Co3/Ni3$(3/4-\epsilon,3/4,\delta)$, and Co4/Ni4$(1/4-\epsilon,3/4,1/2-\delta)$, where ϵ=0.0268 and δ=0.0207 for Co, and ϵ=0.0249 and δ=0.0152 for Ni. The spin-orbit coupling (SOC) term was computed self-consistently inside each atomic sphere, with a radius of 1 Å. The electronic polarization P was calculated using the Berry phase method.[18]

III. MAGNETIC ANISOTROPY: $LiCoPO_4$ VS $LiNiPO_4$

As shown in Fig. 1, each Co ion is surrounded by highly distorted oxygen octahedra, so that the partially filled t_{2g} shell shows a dumbbell-shaped charge distribution, axially elongated along the $\mathbf{n_i}$ direction (along m1-m2 O-Co-O bonds). This peculiar shape is expected to induce a strong local magnetic anisotropy via the SOC term. On the other

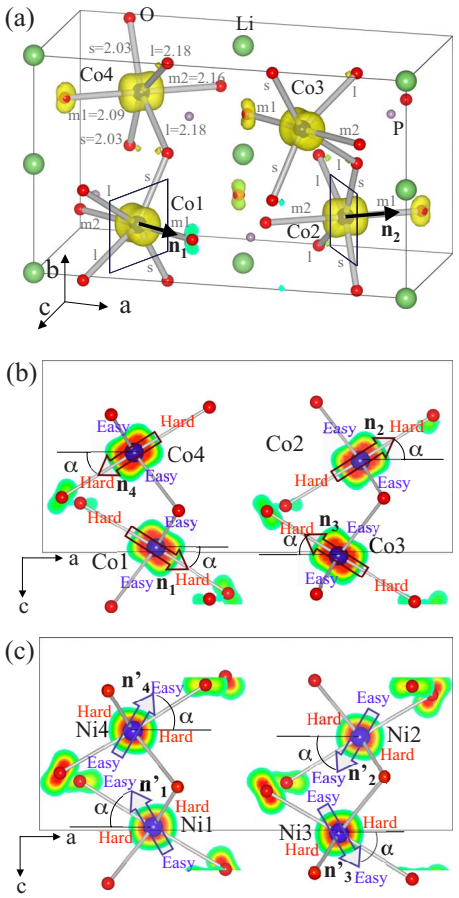

FIG. 1. (Color online) (a) Isosurface of charge density of minority-spin Co-t_{2g} states (within an energy range up to 1 eV below E_F). Co-O bond lenghts (Å) are reported and denoted as $l,m1,m2,s$. Easy planes for Co local spins and the corresponding normal vectors (magnetic "local" hard axis) $\mathbf{n_i}$ are also shown at Co1 and Co2 sites. (b) Section of charge density of Co t_{2g} electrons and local hard axis vectors $\mathbf{n_i}$ in the ac plane in $LiCoPO_4$. (c) Same as (b) for $LiNiPO_4$, with local easy axis vectors $\mathbf{n_i'}$. At each spin site, the easy/hard spin direction is also shown.

hand, in $LiNiPO_4$, the Ni d^8 orbital shows a more isotropic spherelike shape.

Both the global and local magnetic anisotropy were investigated by rotating four spins simultaneously, keeping a collinear AFM coupling. The *global* magnetic anisotropic energy (MAE) was calculated by differences in the total energy with different spin orientations, whereas the *local* anisotropic energy was evaluated as proportional to the expectation value of the SOC energy: $E_{\mathrm{SOC}}=\langle\frac{1}{c^2}\frac{1}{r}\frac{dV}{dr}l\cdot s\rangle$ (as integrated in each atomic sphere), where c is the velocity of light, r is the radial distance in each atomic sphere, V is the effective potential as a function of r, and l and s are, respectively, orbital and spin operators.[19]

A. *U*-dependence of global magnetic anisotropy

First, let us focus on the global MAE, and on its dependence on the value of the effective Coulomb interaction U. Table I shows the total energy difference of collinear AFM configurations where all spins are parallel/antiparallel to the a, b, or c axis. The U dependence of these same quantities is also shown.

TABLE I. MAE (meV) for $LiCoPO_4$ and $LiNiPO_4$ as a function of U-values. Note here that the atomic structure has been optimized for each U.

$LiCoPO_4$	$U=2$ eV	$U=5$ eV	$U=8$ eV
E_b-E_a	−17.84	−19.59	−21.08
E_c-E_a	−8.14	−9.64	−10.75
$LiNiPO_4$	$U=2$ eV	$U=5$ eV	$U=8$ eV
E_b-E_a	0.84	0.94	1.02
E_c-E_a	−0.17	−0.12	−0.11

For all U values, the global easy axis of Co spins is b axis and of Ni spins is c axis, consistent with the experimental suggestion that Co spins are aligned along the b axis (possibly with a slight rotation) and that Ni spins along the c axis.[9,13] The MAE of Co spins is rather high (more than ten times larger than the orbitally ordered Mn spins in $TbMnO_3$).[20] In particular, larger U values lead to larger anisotropy; in general, in fact, a larger effective Coulomb interaction enhances the orbital disproportionation and the consequently stronger spin orbit coupling.

B. Local magnetic anisotropy and the origin

Here we rotate Co/Ni spins in both ac and ab planes by an arbitrary angle to investigate the "local" magnetic anisotropy; in this case, the hard/easy axis of spins is moved away from lattice vector axes a, b, or c.

Figures 2(a) and 2(b) show both the global and local MAE of Co spins in the ac and ab planes, respectively. Although the global easy axis is still the b direction, as shown by the spin angle dependence of E_{SOC} [cf. Fig. 2(a)], the local easy/hard axial direction depends on each Co site. E_{tot} can be fitted by a conventional quadratic anisotropic term for S_i spins: $D(\mathbf{S_i}/|\mathbf{S_i}|\cdot\mathbf{n_i})^2$, where $\mathbf{n_i}$ is the site-dependent hard axis, described as $\mathbf{n_1}=\mathbf{n_3}=(\cos\alpha,0,\sin\alpha)$ and $\mathbf{n_2}=\mathbf{n_4}=(\cos\alpha,0,-\sin\alpha)$ (see Fig. 1). According to the fitting, $D=7.39$ meV and $\alpha=35.48°$: this implies the hard axis $\mathbf{n_i}$ to be nearly along the $m1$ bond so that Co spins are aligned in an easy plane perpendicular to $\mathbf{n_i}$. In terms of site-dependent anisotropy, we note that the stable AFM spin ordering $S_1=S_2=-S_3=-S_4$ is different from the orbital ordering $L_1=L_3$, $L_2=L_4$, which causes a local anisotropy. In such a configuration, all four spins are allowed to lie in the easy plane *only* when collinear AFM spins are pointing along the b axis. Therefore, the b axis is the easy axis in the collinear AFM configurations for Co spins.

Our results for the local anisotropy in Co d^7 can be interpreted as follows: From the diagonalization of the density matrix in the GGA+U procedure, the minority-spin Co $3d$ levels can be almost (with a coefficient larger than 0.97) described by the cubic harmonic functions d_{yz}, d_{zx}, d_{xy}, d_{z^2}, and $d_{x^2-y^2}$ (energetically ordered), where the local axis z is taken as coincident with the $\mathbf{n_i}$ vector and y is taken along the b axis (the x axis is then automatically determined). Con-

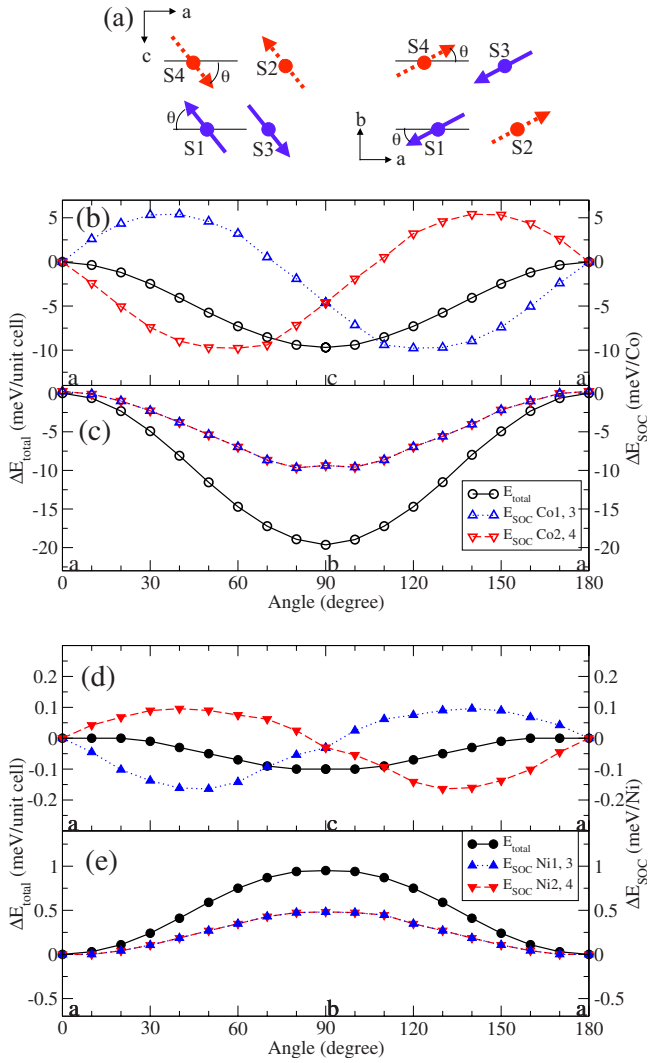

FIG. 2. (Color online) Total energy ΔE_{total} (global magnetic anisotropic energy, denoted by black solid line) and ΔE_{SOC} (local magnetic anisotropic energy, dashed colored lines) at each Co site vs the direction of collinear Co spins (b) in *ac* plane and (c) in *ab* plane, with the collinear spin configuration as shown in (a). The spins {S1, S3} (red dashed arrows) and {S2, S4} (blue solid arrows) are paired due to the corresponding orbital moment direction (see text). Corresponding curves for Ni spins are shown in (d) and (e) for the *ac* and *ab* planes, respectively. Note the different energy scales of panels (b) and (c) compared to (d) and (e). The energy with spins along the *a* axis is taken as reference.

sidering only the minority spin channel, the first two levels are occupied. According to the degenerate perturbation theory[21] and by analogy with Refs. 20 and 22, the largest mixing occurs between unoccupied d_{z^2} and occupied d_{zx} and d_{yz} due to the raising l^+ and lowering l^- operation when the spin lies in the *xy* plane; this minimizes E_{SOC} so that the *z* (i.e., $\mathbf{n_i}$) axis should be the hard axis. On the other hand, at the Ni d^8 state in $LiNiPO_4$, following a similar procedure, the 3*d* levels are described (with a coefficient larger than 0.92) as $d_{x^2-y^2}$, d_{yz}, d_{zx}, d_{z^2}, and d_{xy} (energetically ordered), where the first three levels are occupied. In this case, the magnetic anisotropy cannot be *a priori* predicted.

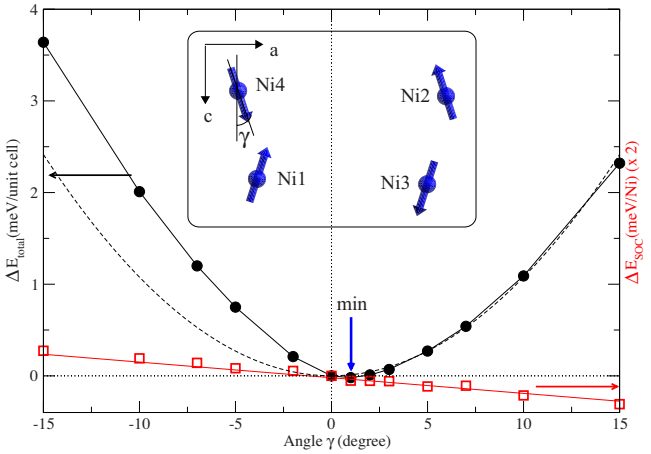

FIG. 3. (Color online) Total energy ΔE_{total} (black solid line) and ΔE_{SOC} (dashed red line) at each Ni site vs the direction of noncollinear Ni spins in the spin-cross configuration (shown in the inset) with angle γ. The minimum is marked by a vertical blue arrow. The dashed line is a function proportional to $1-\cos\gamma$, as a guide to the eye, to outline the "asymmetrical" behavior of the DFT data.

Actually, our calculations show for Ni spins an opposite trend of E_{SOC} to Co spins, with respect to the Co spin, both in the *ac* and *ab* planes (cf. Fig. 2); moreover, the MAE is almost two orders of magnitude smaller, consistent with the spherical d^8 electronic cloud. Here, the *b* axis is the global hard axis. Assuming the easy axis to lie in the *ac* plane and by fitting E_{tot} to the anisotropic term, we estimate $D=-0.50$ meV and $\alpha=46.7°$. Here α is close to $\pi/4$ so that two opposite contributions from local anisotropy nearly cancel out [Fig. 2(c)] and induce a small in-plane anisotropy.

The negative value of *D* implies the existence of an easy axis $\mathbf{n}_\mathbf{i}'$ of Ni spins in the *ac* plane (see Fig. 1), $\mathbf{n}_\mathbf{1}'=\mathbf{n}_\mathbf{3}'=(-\sin\alpha,0,\cos\alpha)$ and $\mathbf{n}_\mathbf{2}'=\mathbf{n}_\mathbf{4}'=(\sin\alpha,0,\cos\alpha)$. Therefore, the *c* axis is the global easy axis for Ni spins if a collinear AFM configuration is assumed. However, in order to stabilize the local anisotropic term, the spins are expected to slightly tilt with respect to the *c* axis. This deviation, denoted as angled-cross spin configuration, has been already discussed by Chupis[11] in terms of Landau theory and suggested to play an important role for magnetoelectricity. This issue has been carefully investigated here by tilting the spins by an angle γ from the *c* axis. Indeed, as shown in Fig. 3, the noncollinear spin structure in the *ac* plane with $\gamma\sim1°$ gives the lowest energy. Therefore, we verified by means of DFT simulations, that the spin-crossed configuration, suggested by Chupis[11] in his Landau model to explain the ME effect, is indeed the ground state of Ni spins.

We considered a generic Hamiltonian for $\mathbf{S_i}$ ($i=1-4$) spins, including a Heisenberg term, a relativistic anisotropy term and a Zeeman-like term (see next paragraph, where a finite external $\mathbf{H}$ field will be introduced),

$$\mathcal{H}=\sum_{\langle i,j\rangle}J_{ij}\frac{\mathbf{S_i}\cdot\mathbf{S_j}}{|\mathbf{S_i}||\mathbf{S_j}|}+\sum_i D\left(\frac{\mathbf{S_i}}{|\mathbf{S_i}|}\cdot\mathbf{n_i}\right)^2+\sum_i\mathbf{S_i}\cdot H. \quad (1)$$

In this $H=0$ case, a delicate balance of the first two terms occurs: As the spin is tilted toward the local easy axis, the

SOC-term is stabilized, whereas the J_{ij} coupling becomes unstable. As a result, the equilibrium occurs in a noncollinear angled-cross spin configuration.

IV. MAGNETOELECTRICITY IN $LiNiPO_4$

The existence of a local magnetic anisotropy is particularly important in the context of magnetoelectricity. In order to investigate ME effects in $LiNiPO_4$, hereafter we focus on the change in the spin configuration under a magnetic field with respect to the angled cross ground state. The exchange coupling constants J_{ij} were evaluated by total energy differences fitted to Eq. (1), considering several AFM configurations. Our calculated values are $J_{12}=J_{34}=-0.118$ meV, $J_{13}=J_{24}=1.46$ meV, and $J_{14}=J_{23}=3.92$ meV (the positive sign means AFM coupling). The dominant J_{14} keeps the spins in the AFM configuration, whereas J_{12} and J_{13} are responsible for removing the degeneracy of some AFM configurations,[9] i.e., the AFM spin configuration $S_1=S_2=-S_3=-S_4$ gives the most stable energy. The J values are consistent with the fact that four Ni sites are separated into two pairs (Ni1, Ni4) and (Ni2, Ni3) by a Li intercalated layer, so that different pairs are expected to be weakly coupled. The anisotropy coefficient D is also obtained from DFT, as reported above. A nonzero applied magnetic field, H_x, is expected to tilt the Ni spins from the angle-crossed spin configuration, with angles from the c axis, denoted as θ_1 and θ_2.[23] (Here, we assume the relation $\theta_1=\theta_4$ and $\theta_2=\theta_3$ by considering the symmetry under the magnetic field.) By using DFT parameters, Eq. (1) is easily minimized by Newton method with θ_1 and θ_2 angles varying by few degrees in a way proportional to H_x [cf. Fig. 4(b), inset].

Constraining the spin angles as obtained from the Newton minimization for each H-field, we evaluate the electronic polarization. A small but finite P_z is obtained, confirming magnetoelectricity. As shown in Fig. 4, all spins have positive x components for $H_x>5T$; however, the sign of the moment doesn't affect the induced P_z, which is rather linearly proportional to H_x, consistent with the experimentally observed behavior at low temperature. From the slope of the P-H curve from $H=0$ to 10 T, the linear ME coefficient α_{zx} is estimated as 0.59 $\mu C/m^2$ T=0.74 ps/m, comparable with the low-temperature experimental value $\alpha_{zx}^{exp}=1.5$ ps/m (Ref. 24) We remark that our results show the linear ME effect to be based on the angle- crossed Ni spins; on the other hand, we cannot explain the ME effect in $LiCoPO_4$ because Co spins are stable in a collinear configuration according to our DFT simulations. Therefore, some alternative mechanisms should be invoked for the Co-based phosphate; this will be the object of future studies.

V. MECHANISM OF EXCHANGE-COUPLING-INDUCED POLARIZATION

Let us now investigate the microscopic origin of magnetoelectricity. Electric dipoles are found to be mainly induced by symmetric exchange,[25] often referred to as "inverse" Goodenough-Kanamori (iGK) interaction[26] in Ni1-O-Ni4 (or Ni2-O-Ni3) bonds. According to the mechanism, the electron

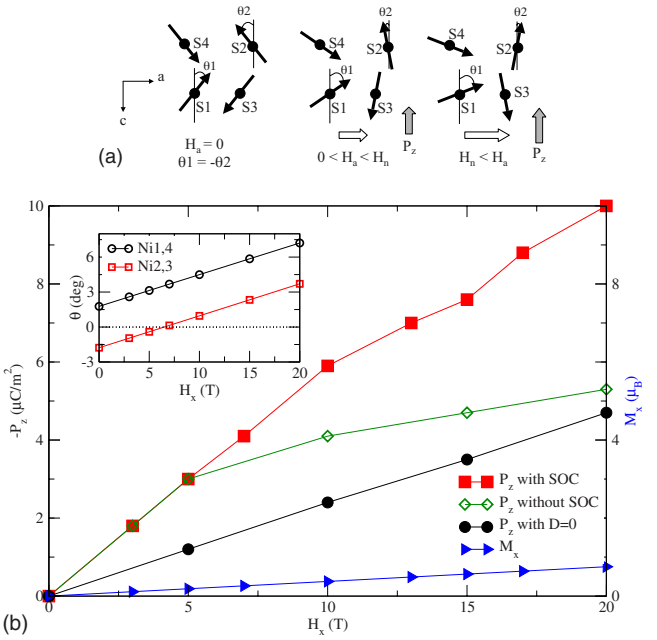

FIG. 4. (Color online) (a) Spin configuration in the ac plane under an applied field H_x. (b) Magnetic-field induced electric polarization along z (with and without SOC, as well as considering $D=0$ in Eq. (1), see text) in $LiNiPO_4$. The magnetization M_x is also shown (left-triangles, referred to the right y axis) Inset: spin angle $\theta 1$ and $\theta 2$ (in degrees) vs H_x (t).

charge, as well as the ion itself, is shifted so as to increase the magnetic energy gain by changing the Ni-O-Ni angle. Accordingly, such a charge shift is believed to induce a net electric polarization. To highlight the effect, we focus on the difference in charge density around Ni-O-Ni bonds between the almost antiparallel spin configuration (at $H=0$ T) and the more "parallel" configuration (at $H=20$ T). Since $J_{14}=J_{23}$ is the dominant exchange interaction, we focus on the Ni1-O-Ni4 and Ni2-O-Ni3 regions (cf. Fig. 5). We expect that such spin rotation (from $H=0$ to 20 T) might induce the oxygens between Ni atoms to displace. In doing so, the Ni-O-Ni angle would become closer to 180°, therefore gaining a

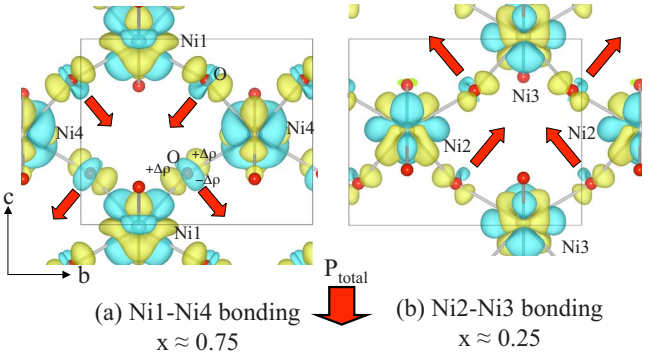

FIG. 5. (Color online) An isosurface of charge density difference (yellow:+,blue:−) between the spin configurations with $H=20$ T and $H=0$ T with fixed atomic structure. (a) Ni1-O-Ni4 bonding and (b) Ni2-O-Ni3 bonding are highlighted. The dipole caused by the shift of charge due to exchange striction and net polarization P_{total} are shown by red arrows.

larger exchange coupling energy. Although the atomic optimization with such small energies involved for noncollinear calculations goes beyond the scope of this work, our guess is supported by the shift of the gravity center of the charge density from the oxygen atomic center (cf. Fig. 5). We remark that, due to the oxygen location with respect to the Ni-Ni bond center, the induced electric dipoles are opposite at Ni1-O-Ni4 and Ni2-O-Ni3 bonds. However, the difference between θ_1 and θ_2 (see main text) prevents the full cancellation, so that a finite P_z arises.

For small H, the other conventional mechanism for magnetically induced polarization—related to antisymmetric exchange and often labeled as "inverse Dzyaloshinskii-Moriya (iDM)"[27] (according to Ref. 24, DM interaction as well as superexchange interaction are important to explain the ME effect in $LiNiPO_4$.)—is negligible. However, for high-magnetic fields, the iDM becomes sizeable [cf. Fig. 4(b)], where the comparison between P_z values including—or not—the SOC term is reported). In this context, we note that the existence of a local anisotropic term is important to induce P: Assuming $D=0$ in Eq. (1), so that $\theta 1=\theta 2$, we find that the induced P_z is less than half with respect to the nonzero D case [cf. Fig. 4(b)].

Finally, we estimate toroidal moments based on Ref. 5. The collinear AFM spin configuration in $LiCoPO_4$ induces $(0,0,-1.52)\mu_B$ Å, whereas the noncollinear spin configuration (at $H=0$ T) in $LiNiPO_4$ induces $(0.19,0.94,0)\mu_B$ Å per unit cell. We observe that the spin-crossed state causes a small T_x-component; however, the T_y component, coming from the compensated AFM spin configuration, is relevant to the ME effect with finite P_z and H_x.

In conclusion, we have presented a careful investigation of the spin-anisotropy in Li-based transition-metal phosphates. We found that $LiNiPO_4$ shows a peculiar ground-state spin configuration: due to a site-dependent magnetic anisotropy, it shows noncollinear spins arranged as angled-cross-like. This is relevant in the context of magnetoelectricity: due to the ground-state noncollinearity, the spin-configuration induced by an applied magnetic field leads to a net electric polarization, as shown by a realistic first-principles estimate of the magnetoelectric coefficient in agreement with experiments. Our results suggest a possible avenue for elucidating the origin of the ME effects in other compounds.

ACKNOWLEDGMENTS

We thank Claude Ederer for helpful discussions. The research leading to these results has received funding from the European Research Council under the EU Seventh Framework Programme (Grant No. FP7/2007–2013)/ERC Grant Agreement No. 203523. Computational support from Caspur Supercomputing Center (Rome) and Cineca Supercomputing Center (Bologna) is gratefully acknowledged.

*silvia.picozzi@aquila.infn.it

[1] K. Amine, H. Yasuda, and M. Yamachi, Electrochem. Solid-State Lett. **3**, 178 (2000).
[2] O. Le Bacq, A. Pasturel, and O. Bengone, Phys. Rev. B **69**, 245107 (2004).
[3] B. B. Van Aken, J. P. Rivera, H. Schmid, and M. Fiebig, Nature (London) **449**, 702 (2007).
[4] H. Schmid, J. Phys.: Condens. Matter **20**, 434201 (2008).
[5] C. Ederer and N. A. Spaldin, Phys. Rev. B **76**, 214404 (2007).
[6] N. A. Spaldin and M. Fiebig, Science **309**, 391 (2005).
[7] M. Mercier, Rev. Gen. Electr. **80**, 143 (1971).
[8] R. P. Santoro, R. E. Newnham, and S. Nomura, J. Phys. Chem. Solids **27**, 655 (1966).
[9] D. Vaknin, J. L. Zarestky, L. L. Miller, J.-P. Rivera, and H. Schmid, Phys. Rev. B **65**, 224414 (2002).
[10] R. P. Santoro, D. J. Segal, and R. E. Newman, J. Phys. Chem. Solids **27**, 1192 (1966).
[11] I. E. Chupis, Low Temp. Phys. **26**, 419 (2000).
[12] J.-P. Rivera, Ferroelectrics **161**, 147 (1994).
[13] I. Kornev, M. Bichurin, J.-P. Rivera, S. Gentil, H. Schmid, A. G. M. Jansen, and P. Wyder, Phys. Rev. B **62**, 12247 (2000).
[14] G. Kresse and J. Furthmüller, Phys. Rev. B **54**, 11169 (1996).
[15] P. E. Blöchl, Phys. Rev. B **50**, 17953 (1994).
[16] V. I. Anisimov, F. Aryasetiawan, and A. I. Lichtenstein, J. Phys.: Condens. Matter **9**, 767 (1997).
[17] I. Abrahams and K. S. Easson, Acta Crystallogr., Sect. C: Cryst. Struct. Commun. **49**, 925 (1993).
[18] R. D. King-Smith and D. Vanderbilt, Phys. Rev. B **47**, 1651 (1993); R. Resta, Rev. Mod. Phys. **66**, 899 (1994).
[19] J. Kübler, *Theory of Itinerant Electron Magnetism* (Oxford Science Publications, New York, 2000).
[20] H. J. Xiang, Su-Huai Wei, M.-H. Whangbo, and Juarez L. F. Da Silva, Phys. Rev. Lett. **101**, 037209 (2008).
[21] D. Dai and M.-H. Whangbo, Inorg. Chem. **44**, 4407 (2005).
[22] H. J. Xiang, Su-Huai Wei, M.-H. Whangbo, Phys. Rev. Lett. **100**, 167207 (2008).
[23] The effect of an applied magnetic field is taken into account only through local spin directions (i.e., neglecting dynamical effects by the field).
[24] T. B. S. Jensen, N. B. Christensen, M. Kenzelmann, H. M. Rønnow, C. Niedermayer, N. H. Andersen, K. Lefmann, J. Schefer, M. v. Zimmermann, J. Li, J. L. Zarestky, D. Vaknin, Phys. Rev. B **79**, 092412 (2009).
[25] S. Picozzi, K. Yamauchi, B. Sanyal, I. A. Sergienko, and E. Dagotto, Phys. Rev. Lett. **99**, 227201 (2007); S. Picozzi and C. Ederer, J. Phys.: Condens. Matter **21**, 303201 (2009).
[26] K. Yamauchi and S. Picozzi, J. Phys.: Condens. Matter **21**, 064203 (2009).
[27] H. Katsura, N. Nagaosa, and A. V. Balatsky, Phys. Rev. Lett. **95**, 057205 (2005); I. A. Sergienko and E. Dagotto, Phys. Rev. B **73**, 094434 (2006); M. Mostovoy, Phys. Rev. Lett. **96**, 067601 (2006).